



NIRCAM – Imaging FTS

Near-Infrared Imaging Fourier Transform Spectrometer for NGST

NGST – DSS – WHRP – 003

October 1, 1999

Work performed under ESA contract for the
“Study of Payload Suite and Telescope for NGST”

ESTEC/Contract no. 13111/98/NL/MS

Table of Contents

0	INTRODUCTION.....	3
1	SCIENCE.....	5
1.1	SUMMARY.....	5
1.2	THE NASA DESIGN REFERENCE MISSION (DRM).....	5
1.2.1	DRM overview.....	5
1.2.2	Cosmology and the Structure of the Universe.....	6
1.2.3	Origin and Evolution of Galaxies.....	7
1.2.4	The History of the Local Universe.....	7
1.2.5	Birth of Stars.....	8
1.2.6	Origin and Evolution of Planetary Systems.....	8
1.2.7	Clustering and Proto-Clusters in the early universe.....	9
1.3	IMAGING FTS TECHNICAL SPECIFICATIONS.....	10
1.3.1	Instrument Performance Requirements.....	10
1.3.2	Instrument Operations.....	11
2	ENGINEERING.....	13
	NOTE: DETAILS ON MECHANICAL, THERMAL AND ELECTRICAL DESIGN CAN BE FOUND IN REF. /3/.....	13
2.1	DESIGN CONCEPT.....	13
2.1.1	Interferometer.....	13
2.1.2	Optical Design Description.....	17
2.1.3	Optical Performance.....	19
2.1.4	Photometric Performance.....	25
2.1.5	Opto-Mechanical Design.....	26
2.1.6	Budgets.....	27
2.1.7	Conclusions.....	28
2.2	CRITICAL AREAS AND RECOMMENDED DEVELOPMENT ACTIVITIES.....	29
2.2.1	Instrument Hardware Breakdown.....	29
2.2.2	Critical Areas and Technology Requirements.....	29
2.2.3	Recommended Follow-On Activities.....	31
2.2.4	Technology Development Roadmap.....	31
2.3	DEVELOPMENT PLANNING FOR PHASES B AND C/D.....	33
2.3.1	Work Breakdown Structure.....	33
2.3.2	Development Planning.....	34
2.3.3	Schedule.....	36
3	REFERENCES.....	37

0 INTRODUCTION

As part of its Origins program, NASA is currently undertaking definition and feasibility studies of a Next Generation Space Telescope (NGST) to succeed the Hubble Space Telescope (HST) after 2005. NGST is foreseen to have an aperture of 8 meters and be optimized for near infrared wavelengths (0.6 - 10+ microns) in order to enable the exploration of the most remote high redshift universe.

NASA has invited ESA to extend their successful collaboration on HST to the NGST project, and a draft agreement concept is in place which aims at securing European participation in NGST at a similar level as on HST. ESA has undertaken a number of assessment studies which aimed at defining its potential instrument and spacecraft hardware contributions to the mission.

One of these ESA studies called “Study of Payload Suite and Telescope for NGST” (ref. /1/), has been conducted by Dornier Satellitensysteme GmbH (DSS), Ottobrunn, together with Alcatel Space (AS), Cannes, and a team of 16 European science institutes chaired by Laboratoire d’Astronomie Spatiale, Marseille, and UK Astronomy Technology Centre, Edinburgh. DSS took the responsibility for the overall study and the payload, AS for the telescope, and the science team was responsible for the instrument and telescope definition and requirements.

The **NIRCAM – Imaging FTS** is one of four instruments that were defined by the science team as potential NGST payload and was detailed by DSS.

This document contains the instrument opto-mechanical design and analyses and the instrument specific development planning. Technical aspects that are common to all payloads studied by DSS (NIRCAM-FW, NIRCAM-FTS, MIRCAM, MIRIFS and IFMOS, which was studied under a separate contract) are described in a separate report, ref. /3/. These aspects include

- optical interface
- material selection, mechanisms
- thermal design and analysis
- electrical design, detectors, data processing
- common critical areas

Payload Study Team

ESA:

NGST study manager	J. Cornelisse
NGST study scientist	Dr. P. Jakobsen

Dornier Satellitensysteme:

Study mgmt., system engineering	W. Posselt
Optical engineering	Dr. W. Holota, P. de Zoeten
Mechanical engineering	D. Scheulen, H. Huether
Thermal engineering	A. Hauser
Electrical eng., data processing	W. Hupfer
Focal plane arrays	Dr. R. Buschner-Ueberreiter

Science Team:

Laboratoire d'Astronomie Spatiale	Dr. O. Le Fèvre
UK Astronomy Technology Centre	Dr. G. Wright

Chairing a consortium of the following institutes:

- Observatoire de Lyon
- European Southern Observatory
- Leiden Sterrewacht
- University of Durham
- University of Cambridge, Institute of Astronomy
- Max-Planck-Institut für Extraterrestrische Physik
- Observatoire de Haute Provence
- Rutherford Appleton Laboratory
- Max-Planck-Institut für Astronomie
- Astrophysikalisches Institut Potsdam
- Instituto de Astrofísica de Canarias
- University of Leicester
- Institut d'Astrophysique de Paris
- Service d'Astronomie, CEA-Saclay

BOMEM, Canada:

Technical consultant	A. Villemaire, J.F. Legault
----------------------	-----------------------------

1 SCIENCE

1.1 Summary

An imaging FTS would be capable of carrying out a great many of the programmes in the DRM, namely all those which require imaging and/or low spectral resolution wide field/multi-object spectroscopy. We review the DRM science areas, describing the relevance of an imaging FTS. Required instrumental capabilities are then derived from the science goals.

1.2 The NASA Design Reference Mission (DRM)

1.2.1 *DRM overview*

The NASA Design Reference Mission has been defined with the goal to identify the most promising science NGST can do, and to help set the science requirements defining the instrument payload. A large fraction of the NGST mission is a core program, designed to understand the origin and evolution of galaxies, mapping dark matter, measuring cosmological parameters and study the physics of star formation. The DRM also includes a range of other studies which fall within the NASA Origins program. The studies in the DRM are being defined to a level of detail which includes the number density and brightness of potential targets, the number of observations needed and the desired observing modes. The DRM has been divided into five broad science areas: Cosmology and the Structure of the Universe; Origin and Evolution of Galaxies; The History of the Local Universe; Birth of Stars; Origin and Evolution of Planetary systems. The programs covered by these science areas are reviewed below. The goal is for the NGST to be capable of accomplishing the studies in the DRM in less than 3 years.

Table 1.2-1 presents the current list of DRM programs, as ranked by the NASA-ASWG.

An important issue is that the DRM does not represent all of the science that will be done by NGST, and since it is difficult to anticipate in detail the most important studies at the time of launch, some flexibility in the instruments is required. An FTS can provide some of this in the form of variable spectral resolution, and in its ability to carry out spectroscopic surveys un-biased by selection effects. We outline some of the DRM programs of which an imaging FTS would be capable below.

Rank	Score	SDM	DRM Title
1	1.9	0.4	Form. & Evol. Galaxies- Imaging
2	2.9	0.4	Form. & Evol. Galaxies- Spectra
3	6.2	0.9	Mapping Dark Matter
4	6.8	0.8	Searching for the Reionization Epoch
5	7.3	0.9	Measuring Cosmological Parameters
6	7.8	1.0	Form. & Evol. Galaxies- Obscured Starform. & AGN
7	8.4	1.0	Physics of Star Formation: Protostars
8	10.5	1.0	The Age of the Oldest Stars
9	11.3	1.4	Detection of Jovian Planets
10	11.8	1.5	Evolution of Circumstellar Disks
11	12.0	1.5	Measuring the Rates of Supernovae
12	12.1	1.1	Origins of Substellar Mass Objects
13	12.2	1.2	Form. & Evol. Galaxies- Clusters
14	13.9	1.3	Form. & Evol. Galaxies near AGN
15	14.1	0.8	Cool Field Brown Dwarf Neighbors
16	14.6	1.1	Survey of Trans-Neptunian Objects
17	16.0	1.4	Properties of KBOs
18	16.8	1.0	Evolution of Organic Matter in ISM-Astrobiology
19	17.0	1.1	Microlensing in the Virgo Cluster
20	17.0	0.9	Ages and Chemistry of Halo Pops.
21	17.6	0.9	Cosmic Recycling in the ISM
22	18.5	0.8	IR Transients from GRBs and Hosts
23	18.7	0.9	IMF for Old Stellar Populations

Table 1.2-1: Ranked list of DRM programs (from NASA-ASWG). The core programs 1-7 are shaded

1.2.2 Cosmology and the Structure of the Universe

Measuring the distribution of dark matter in the universe is crucial for understanding the evolution of structure since the Big Bang, and for understanding the nature of dark matter. By using weak gravitational lensing techniques to analyse ultra-deep multi-band images the dark matter distribution can be determined on scales ranging from individual galaxies, through groups and clusters up to the large scale (3Mpc) matter distribution. The combination of imaging observations and spectroscopic information on the brightest members will allow to investigate the relationship between dark and visible matter on large scales. An IFTS can carry out both narrow band imaging (for multiple bands) and low spectral resolution spectroscopy over wide fields simultaneously, and is thus capable of carrying out these surveys in an efficient manner. (The lower sensitivity for narrow band imaging due to the need to scan the FTS being compensated by using the spectral information as well).

NGST will be uniquely capable of both discovering and obtaining spectroscopy for distant supernovae (SN) at redshifts of 2-4. Type 1a supernovae can be used as standard candles to directly study the geometry of the universe. q_0 , Λ and Ω can be

determined from measurements of apparent magnitude as a function of redshift, and as the redshifts get higher the magnitude difference differentiating cosmological models increases, and thus supernovae at redshifts 2-4 will yield more definitive cosmology results than ground based surveys. In addition finding the “turn-on” redshift of type 1 SN from deep searches is important for understanding the chemical evolution of galaxies since they are the major source of iron production. Deep wide field images will play a key role in finding distant supernovae, but identifying the sources as SN and determining the SN type will also require low resolution wide band-width spectroscopy. SN searches will thus require wide field surveys with both photometric and spectroscopic information, tasks which could potentially be carried out simultaneously with an imaging FTS.

1.2.3 *Origin and Evolution of Galaxies*

The goals of these programmes are to find the first generation of stars and quasars and to carry out deep imaging and spectroscopic surveys in the near-IR to study galaxy formation and evolution for field and cluster galaxies, the effects of AGN on chemical evolution and to understand the nature of gamma ray burst sources.

Deep observations with NGST are uniquely suited to identifying sources at redshifts of $z > 10$ through their Lyman-alpha break at wavelength $1.2[(1+z)/10]$ microns. This is an important test because various models for structure formation make similar predictions about the local universe but differ significantly in their predictions of the number and distribution of sources at very high redshifts.

The deep imaging surveys are aimed at determining photometric redshifts and morphologies of galaxies. The formation of disks and population II halos can then be traced to high redshifts to study the importance of merging, the relative roles of gravity, dissipation and energy injection on different scales and the interaction between galaxies and the IGM.

The spectroscopic survey will build on the imaging survey results and is aimed at understanding the building of the Hubble sequence over redshifts of 1-15 or more. Spectra will be used to determine cluster membership, star-formation rate, metallicity, reddening and kinematics mass estimates. Masses of galaxies at $z > 1$ are a critical test of cold dark matter cosmology.

This is an area where the deep imaging capabilities of NGST, coupled with spectroscopic information are likely to open new areas of study, based on "serendipitous" discoveries found in the deep iamges.

1.2.4 *The History of the Local Universe*

The studies of the history of the local Universe are based on the determination of the low-mass end of the IMF in globular clusters, very nearby galaxies, chemical evolution of halo populations, the IMF of old stellar populations and the ages of stars

in local group galaxies. All require the highest spatial resolutions possible and accurate optical/near-IR photometry.

While massive star-formation can readily be observed from the ground to high red-shifts, low mass stars are currently invisible at distances beyond the LMC. However low mass stars constitute most of the mass and structure of galaxies. The greater sensitivity and resolution of NGST means that it will be possible to determine whether the oldest stars in M31 have the same ages as those in our galaxy. Detections at $R \sim 31$ can reach a 15Gyr old main sequence turnoff out to distances of 1 Mpc. Very long exposures would be capable of establishing ages for the oldest stars in M81 and NGC 5128.

The age of the oldest stars in our galaxy could be determined by using deep high resolution near-IR imaging to determine the absolute magnitude of the end of the white dwarf cooling sequence in nearby globular clusters. Such studies are important because they would be the first measurements of the stellar ages which are independent of the main sequence turn-off and stellar evolution theory.

1.2.5 *Birth of Stars*

The studies of the birth of stars included in the DRM are concerned with probing the IMF in star formation regions with a view to determining the origin of distribution of stellar masses. The goal is to compare the low-mass end of the IMF in regions found to be forming stars under a variety of different physical conditions. NGST with its combination of high spatial resolution and low thermal background will be able to sample the emergent mass distributions in young clusters down to planetary mass objects out to 1kpc. Infrared imaging combined with multi-object spectroscopic follow-up will be used to determine whether or not the IMF is universal down to the minimum mass for molecular cloud fragmentation and to characterise the shape of the IMF for 1-20 Jupiter masses i.e. the boundary between planets and stars.

1.2.6 *Origin and Evolution of Planetary Systems.*

Studies of the origin and evolution of planets in the DRM include studies of the Kuiper belt objects in our solar system, direct imaging of planets around nearby stars, and the study of debris disks around stars and proto-stars.

NGST can observe low mass stars in star forming regions out to several kpc, providing the first opportunity to study the detailed properties of proto-planetary disks as a function of age, stellar mass and environment. Combining both near and mid-IR spectroscopy is important to understand the distribution and evolution of the dust and gas in proto-planetary disks. Dust grain sizes, compositions and ice mantles could be studied as a detailed function of radius, vital information for understanding the formation and composition of gaseous planets. For older stars in which active accretion has ceased, mid-IR measurements are essential for the study of optically thin dust disks, the precursors of β -Pic type systems. These studies require both good

photometric imaging and low resolution spectroscopy across the full 1-5 μ m band, as well as in the mid-IR and so an imaging FTS would be suitable for this. (Direct searching for planets close to stars requires a coronagraph, as described elsewhere, and this would be difficult to incorporate in an FTS).

1.2.7 *Clustering and Proto-Clusters in the early universe.*

Understanding the formation and evolution of large scale structures is a long time quest for cosmology. While we have made significant progress and more is expected with the 8-10m class ground based telescopes, the question of the early formation of the most massive structures will remain a cornerstone of cosmological investigations until a complete picture is drawn.

On the largest redshift surveys in our local universe, there is convincing evidence that the distribution of galaxies is inhomogeneous on all scales smaller than 100 Mpc. The distribution remains strongly inhomogeneous even out to $z \sim 1$, with galaxies distributed in another density peaks and empty regions ("picket-fence" distribution).

At redshifts beyond 1, very little is known about large scale structures. Only a few large structures have been identified so far. Significant clustering of galaxies has been observed at $z \sim 3$, still within the predicted range of models such as the CDM. At these redshifts, the prevalence of clusters, proto-clusters, or other large scale structures in the distribution of galaxies, is as yet unknown, and the evolution of structures may well be in a critical stage, where observations can directly constrain cosmological models. It is most probable that the early phases of large scale structures assembly will still remain to be explored after the work from the 8-10m ground based telescopes has levelled down. This is where the NGST is expected to play a unique role.

The goals of this programme are (i) to study the site of formation of clusters of galaxies, "proto-clusters", to establish the morphological and dynamical properties of proto-cluster cores, and of the galaxies in them, and (ii) to establish the clustering properties of the distribution of galaxies at redshifts much larger than 3. The study of ~ 100 (proto-) clusters at high redshifts $z > 3$, will be best done from integral field spectroscopy in a field comparable to the proto-core dimensions, on order 1 arcmin. The study of the clustering properties of galaxies at earlier epochs will be best done from a sample of several tens of thousand redshifts of galaxies, best obtained with a wide field spectrograph with a high multiplex factor (number of simultaneous objects observed).

1.3 Imaging FTS Technical Specifications

The concept of an FTS was felt to be particularly attractive if it were able to combine imaging in broad bands with low resolution spectroscopy up to $R \sim 300$. If the number of instruments in the NGST payload suite is limited, then combining two functions in a single instrument makes efficient use of resources. Depending on the emphasis put on ultimate single source performance vs. survey performances, an imaging FTS is a complementary approach to the NIR camera and the NIR MOS combination.

There are many different options for an imaging FTS, such as whether or not both output ports should be used. We chose for this study to investigate a very simple FTS, which could fully meet the requirements for a camera carrying out deep broad band imaging and also provide a versatile narrow-band imaging and low resolution spectroscopic capability.

1.3.1 *Instrument Performance Requirements*

Our concept for an IFTS is optimised to provide the same performance for broad band imaging, with the same number of detectors, as the near-IR camera which was also part of this study. Since broad band near-IR imaging capability is at the core of so much NGST science we felt that it was important not to compromise it in any way when the FTS is used as a camera. This meant that given the same number of detectors for the FTS as for the camera, to achieve the same field and spatial sampling as the camera a single output port has to be used. Imaging with the same throughput as a simple camera is then achieved by setting the FTS to zero path difference, where constructive interference ensures that all of the light is transmitted to the detector. As with the camera, it was considered important to keep the instrument simple with a fixed spatial sampling. To meet the narrow band imaging requirement of the camera, the images are reconstructed from very low resolution spectra taken by scanning the FTS. This is less efficient than simple imaging with a narrow band filter, but on the other hand it allows any central wavelength to be selected. A consequence of putting all the detectors at one output port is that the FTS is optimised for spectroscopic surveys, not for the best individual source sensitivity of which an FTS is capable. Again with simplicity in mind, provision for only low resolution spectroscopy (R up to ~ 300) was considered.

The primary requirements for the NIR FTS are thus that it should have at least as large a field as the near-IR camera with the same spatial sampling and the same broad band filter set. In addition it should provide low resolution spectroscopy (by scanning of the FTS), and narrow band imaging (by summing spectro-images). No requirement was placed on including the camera narrow band filter set in the FTS because of the added complexity.

The final high level requirements for the FTS are as given in Table 1.3-1.

Instrument	Item	Specification
NIR-FTS	Wavelength Range	0.6 – 5 μ m
	Field of View	3 x 6 arcmin
	Spatial sampling	0.03 arcsec/pix
	Filters	Broad band (..JHK...)
	Resolution	5 to 300
	Detector readout	Non destructive readout
	Sensitivity	Same as camera in broad band imaging mode

Table 1.3-1: High level specifications for the NIR FTS

1.3.2 Instrument Operations

The FTS will have the following operating modes :

Broad Band Imaging - simple and surveys

FTS scan mechanism is set to zero path difference and selected broad band filter is inserted. Repeated exposures are summed to produce the required S/N. Jittering and “drizzling” techniques may be used to ensure the best spatial resolution and remove bad pixels.

For surveys the telescope may be stepped through several positions with an image taken at each, to map a larger area than the field of view in the chosen band. For each position jittering and “drizzling” techniques may be used to ensure the best spatial resolution and remove bad pixels. The images will be pasted together into larger mosaics during data reduction which requires any optical distortion to be stable and well calibrated.

For many programs observations will be obtained through more than one broad band filter at each telescope pointing position.

Narrow Band Imaging

FTS is scanned far enough for the desired image band-width (e.g. to simulate a 1% filter the FTS should be scanned over a distance corresponding to $R = 100$), with a broad band blocking filter used to limit the total band pass to reduce the background. Repeated scans are summed to produce the required S/N and “jittering/drizzling” between FTS scans may be used.

An image at the appropriate wavelength and bandpass is reconstructed in the data reduction by summing the data over the required range, after the inverse-Fourier transform stage. Bad-pixel and cosmic ray removal is carried out in Fourier space, so

that clean images result. More than one such “equivalent narrow band image” may be derived from a single FTS scan observation.

The telescope may be stepped through several positions with FTS scans and jittering taken at each telescope position to map a larger area in the chosen band.

Low Resolution Spectroscopy

This is the same as for narrow band imaging, except that the spectral resolution will be selectable up to $R = 300$, and the spectral information will be kept at the data reduction stage.

The telescope may be stepped through several positions with FTS scans taken at each to obtain spectroscopy for a larger survey area than the instrument field of view.

Flat Field Calibrations

These will be derived by median filtering of jittered sky images obtained with the appropriate broad band filter selected and the instrument in broad band imaging mode, or spectroscopy mode as appropriate.

Photometric Calibrations

These will be obtained by observation of sources of known magnitude in either the broad band imaging mode or spectroscopic mode.

Wavelength Calibration

Wavelength calibration will be confirmed by observation of known sources of unresolved emission lines – such as planetary nebulae. Absolute wavelength calibration is intrinsic to the FTS mechanism.

2 ENGINEERING

Note: details on mechanical, thermal and electrical design can be found in ref. /3/.

2.1 Design Concept

2.1.1 Interferometer

Interferometer Optical Design

The interferometer optics is a dual input / dual output Mach-Zehnder configuration, although in the actual instrument design only a single output port will be used. Its principle design is shown in Figure 2.1-1.

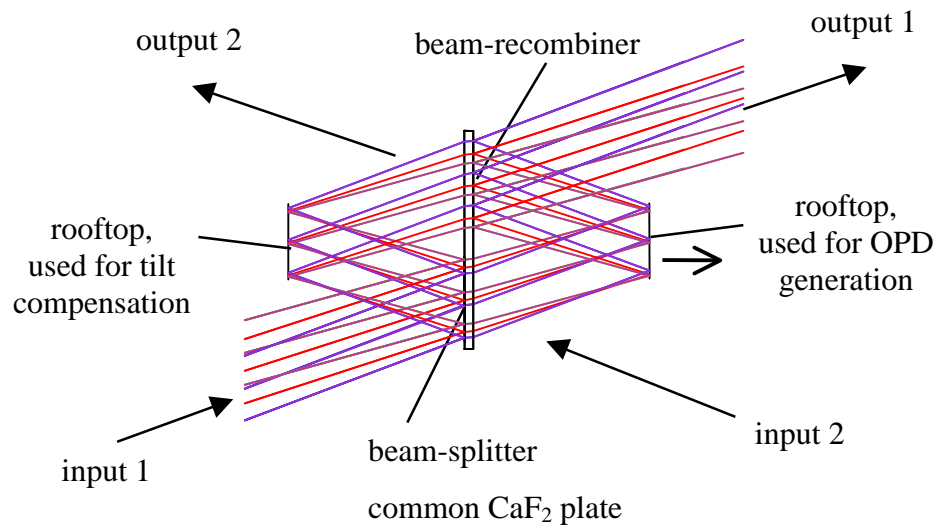


Figure 2.1-1: Interferometer optical design

The interferometer optics consist of

- a CaF_2 -plate with beam-splitting coating at the input and a beam-recombining coating at the output
- a fixed and a moving retro-reflector

The beamsplitter and the beam-recombiner are on opposite sides of the same CaF_2 substrate, and both coatings have identical designs.

Rooftops are preferred as retro-reflectors rather than plane mirrors, since they are insensitive to small tilt angles around the rooftop intersection line and require tilt control only around the axis perpendicular to this paper plane. Plane mirrors require tilt control around both axes. (The effect of tilt of the two recombined wavefronts is described in the chapter about modulation efficiency.)

Principle of Operation

The input radiation is amplitude divided by the beam-splitter. A variable, time dependent Optical Path Difference (OPD) is introduced between the two parts of the divided input beam by mechanical movement of one (or both) retro-reflector(s). Then, both parts of the input beam are recombined at the beam-recombiner and thus brought to interference: the time dependent OPD variations result in intensity fluctuations at the focal plane due to constructive and destructive interference, creating a time dependent signal amplitude at each detector pixel. Inverse Fourier transformation of the interferometric signal retrieves the original spectrum with a spectral resolution that depends on the maximum OPD between the two beams.

The imaging performance of the optical system is not affected by the interferometer mode, i.e. the full spatial information of the camera mode will also be available in the interferometer mode.

Camera Mode

In the camera mode, the optical path difference is kept at zero (both retro-reflectors are in default position). This results in constructive interference of all input radiation in the symmetrical output port 1 (the port with one transmission and one reflection at the beam-splitter/beam-recombiner), and destructive interference of all input radiation in the non-symmetrical output port 2 (two transmissions or two reflections). In this mode the interferometer is optically not present and the efficiency is similar to a broad band filter wheel camera.

Second Input and Output Port

The radiation incident at both input ports is mixed in the interferometer and results in the superposition of both input signals at both output ports. Therefore, especially when observing dense object fields, the second input port should only be used for calibration purposes or for an optical reference for OPD measurements.

The second output port, however, contains in interferometer mode the same information as the first port and can thus be used independently from the first port: using the same optics will compensate the factor 2 efficiency loss of a single port interferometer, or using different optics (and different FPAs) will allow to change the spatial resolution and/or the spectral range and do independent science.

In the actual design these enhancement capabilities have not been further detailed, and the second input and output ports are both blocked by plates of high emissivity, thus simulating quasi-zero radiation sources.

Interferometer Operation

One of the rooftops is kept fixed. It will be used to adjust the tilt angle of the recombining wavefronts by slight rotation of the rooftop around the X-axis (perpendicular to the paper plane). The other rooftop is used to generate the optical path difference by means of an accurate actuator.

In the baseline concept the retro-reflector is moved from the zero position in one direction only, thus creating “single sided” interferograms. Besides a somewhat lower readout noise contribution this concept has an operational advantage: the IFTS will start to gather broad band image information at ZPD, and the spectral details will increase with increasing OPD (or with time). The measurement of the interferogram can be ceased at any OPD position, and can later on be started at this position again if further spectral information is required (in this latter case a few samples at ZPD will be needed for calibration purposes).

First task when operating the IFTS is thus to determine the ZPD position and to minimize the effect of tilt. In practice this can be an automated sequence searching for the peak of the interferogram when all filters are removed (this will provide a very distinct peak at ZPD) and then find the tilt position for maximum amplitude.

The figure on the right shows the Fourier transform of a broad band Planck function to illustrate the task described above.



Interferometer Design Requirements

The interferometer opto-mechanical design is shown in Figure 2.1-2; indicated are important mechanical design requirements.

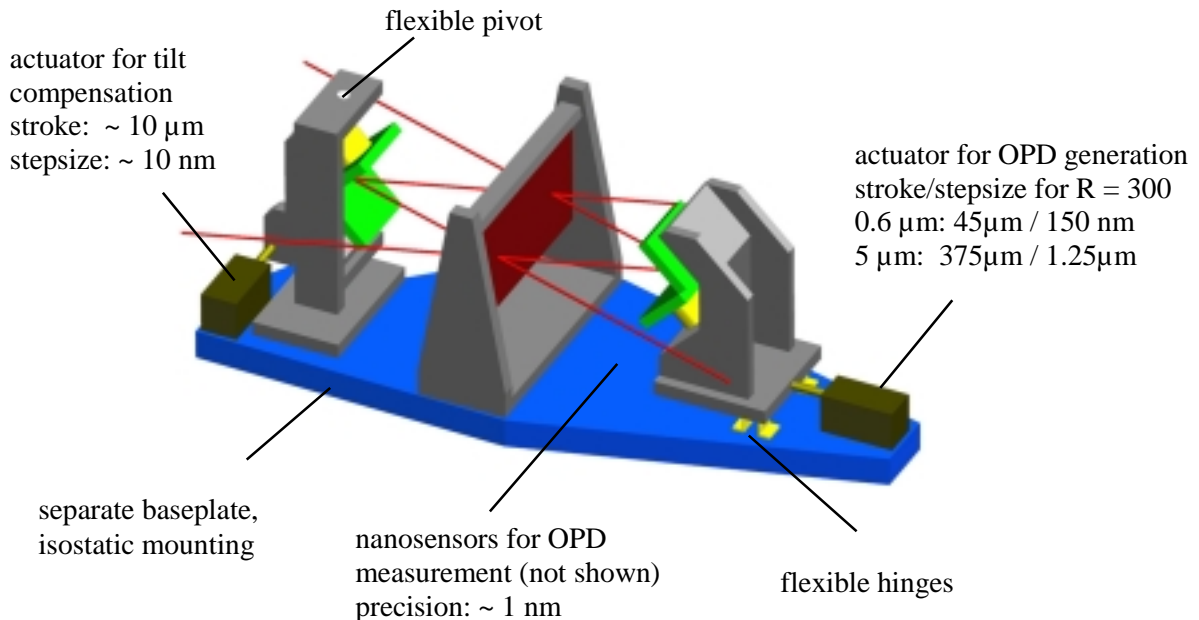


Figure 2.1-2: interferometer opto-mechanical design

For the required resolving power of $R = 300$ the nominal mechanical stroke of the retro-reflector is $375 \mu\text{m}$ at $5 \mu\text{m}$ wavelength. The necessary stroke at the lower wavelength edge of $0.6 \mu\text{m}$ is reduced by the ratio of the wavelengths. The same ratio applies for the stepsize, which is $1.25 \mu\text{m}$ at $5 \mu\text{m}$ and 150nm at $0.6 \mu\text{m}$. Although the Mach-Zehnder configuration introduces shear during OPD acquisition, the optical design tolerates a mechanical stroke of several mm without significant performance degradation.

The required tilt accuracy is $0.5 \mu\text{rad}$, and can be achieved by means of a piezo-electric drive with about 10nm stepsize and $10 \mu\text{m}$ stroke.

The OPD measurement will usually be performed using an optical reference like a laser beam or an LED (for low spectral resolution). However, the coupling of the laser beam to the cold stage via fibers is critical for the large temperature difference along the fibers, and low temperature LEDs are not yet space qualified. In addition, the reference light should be switched off or blocked during the science measurement, in order to avoid straylight (e.g. by multiple reflections in the beamsplitter unit).

On the other hand, the expected in-orbit thermo-mechanical conditions are much more stable than in any laboratory on ground. An interesting alternative to an optical reference is thus to rely on the mechanical stability of the interferometer and measure the OPD with a mechanical device like e.g. the capacitive nanosensors of Queensgate. The required OPD measurement accuracy is about 1nm ($< 0.5\%$ of the stepsize), which is in the range of capabilities of these sensors.

The thermo-mechanical stability of the interferometer unit can be achieved by isostatic mounting of the unit, providing thermal and mechanical decoupling from the instrument baseplate. The first Eigenfrequency of a C/SiC bench should be well above 200Hz and should thus not be susceptible to residual micro-vibrations. The thermal deformations of a C/SiC bench are also quite small: a variation of the thermal gradient (a 2nd order temperature effect) of e.g. 10mK will elongate the interferometer bench ($\sim 50 \text{cm}$ length) and lead to an insignificant OPD variation of $\leq 1 \text{nm}$. Temperature gradients in the other two directions are even less critical since their effects are compensated by the optical design.

2.1.2 *Optical Design Description*

The optical configuration of the NIRCAM-FTS is based on the scientific performance requirements of Table 1.3-1 and shown in Figure 2.1-3. It is a common design for both the camera and the FTS operation modes. The optics consist of the following functional units

- collimating optics
- filter wheel
- interferometer
- imaging optics.

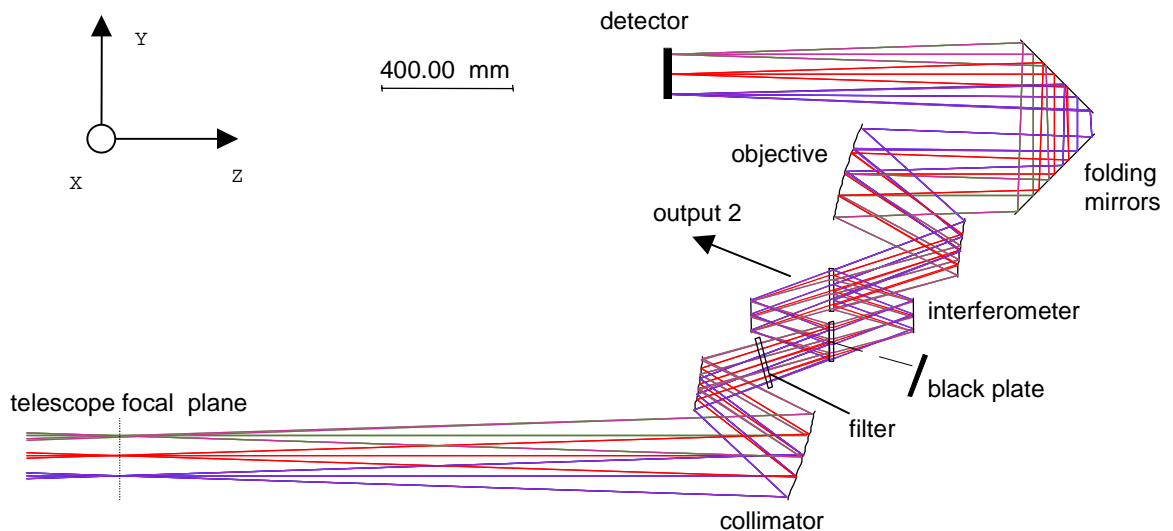


Figure 2.1-3: NIRCAM – FTS optical configuration; the field is 6' x 3' in X/Y direction

Collimating and Imaging Optics

The collimating and imaging optics are slightly different tele-objective designs with focal lengths of 1.7 m. They consist of two aspherical mirrors each, but which are not critical for manufacturing.

The collimating optics have a telecentric entrance pupil. The exit pupil lies about 860 mm behind the second (convex) mirror. Vice versa, the imaging optics have a telecentric exit pupil, and the entrance pupil lies about 860 mm before the first (convex) mirror.

The aperture stop of the system is at the intersection line of the rooftops in the interferometer optics, so that the interferometer part of the system is as compact as possible and can be built and tested as a separate module.

The collimating optics have been optimized to produce a parallel beam of very good quality at the interferometer and to form, together with the imaging optics, a very good 1:1 image of the telescope focal plane at the detector.

Because of the tele-objective designs, the mechanical dimensions are much smaller than the focal lengths. However, the actual dimensions are still rather big due to the required large field and the need for very good image quality over the whole field. Smaller object and image distances would very rapidly decrease the image quality.

Filter Wheel

The filter wheel is located in the parallel beam between the collimating optics and the interferometer optics. The filter wheel contains 8 standard astronomical broad band filters and one empty position. The empty position is useful for alignment purpose and to determine the ZPD position for the camera mode – the interferogram peak will be sharper and more easily be determined if the whole spectrum is used.

Folding Optics

Two folding mirrors arranged under an angle of 45° are used to get the focal plane close to the optics on the common baseplate. These two mirrors are mechanically connected and movable by means of a refocusing mechanism, to focus the beam on the detector array if necessary after cool down.

Table 2.1-1 below summarizes the IFTS design parameters.

Design parameters of NIRCAM-FTS	
Parameter	Value
Wavelength range	1 to 5 μm
Reduction ratio	1
F-number at object side	16
Field (arcmin)	6' x 3'
Detector arrays	12K x 6K
Pixel size	18.5 μm
IFOV	0.14 μrad (or 30 mas)
Entrance pupil	telecentric
Exit pupil	telecentric
Stop	at rooftops
Stop diameter	100 mm
Beam-splitter and beam-recombiner	On one CaF ₂ plate, identical coating designs
Spectral Filters	Filter wheel with 8 broad band filters and one blank position

Table 2.1-1: NIRCAM – FTS design parameters

2.1.3 *Optical Performance*

Image Quality and MTF

The optical performance of the image (at the detector) is diffraction limited. The wavefront errors and Strehl ratios are given in Table 2.1-2 for the center position and the extreme field positions.

Wavefront error of NIRCAM - FTS and Strehl ratios calculated for a wavelength of 1 μm .			
Relative field position (X, Y)		Wavefront rms	Strehl ratio
0	0	0.058	0.87
1	1	0.062	0.86
-1	1	0.062	0.86
1	-1	0.069	0.83
-1	-1	0.069	0.83

Table 2.1-2: NIRCAM – FTS wavefront errors and Strehl ratios at detector

The MTF as a function of frequency is given in Figure 2.1-4. At all field positions the MTF is fairly close to the diffraction limit.

The MFT as a function of defocusing (through-focus MTF) for a spatial frequency of 15 cycles/mm is given in Figure 2.1-5. A defocusing of 0.25 mm gives a maximum decrease in MTF of about 13%.

Figure 2.1-6 gives the spot diagrams of the images at the detector for the center and the corners of the field. Figure 2.1-7 shows the lateral geometric aberrations at the detector.

Figure 2.1-8 shows the planarity of the wavefronts in the interferometer for several field angles and expressed in fractions of the reference wavelength of 1 μm . The performance at the center and the corners of the field is shown.

The field angles of all figures are expressed in relative coordinates w.r. the maximum field angles.

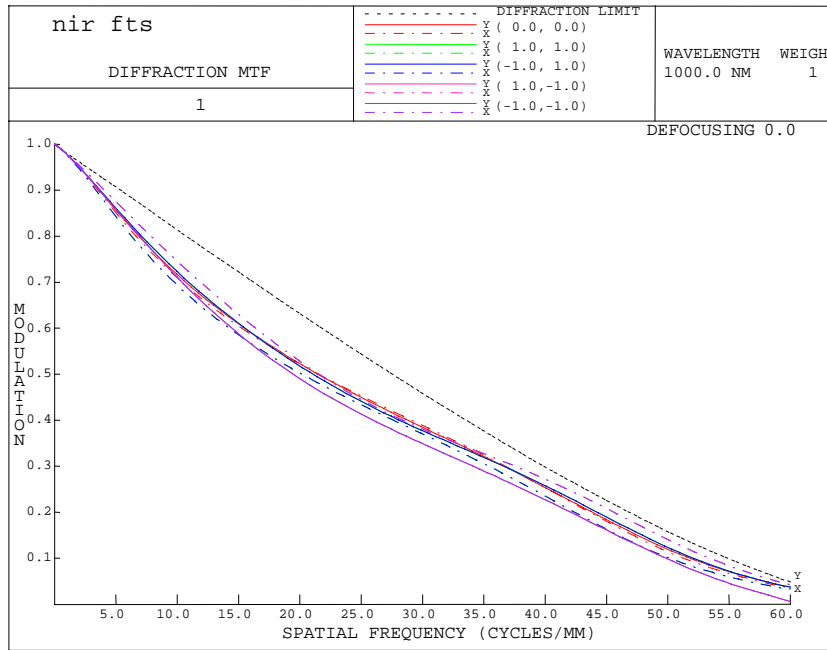


Figure 2.1-4: NIRCAM-FTS: MTF as a function of spatial frequency calculated in center and corners of the field.

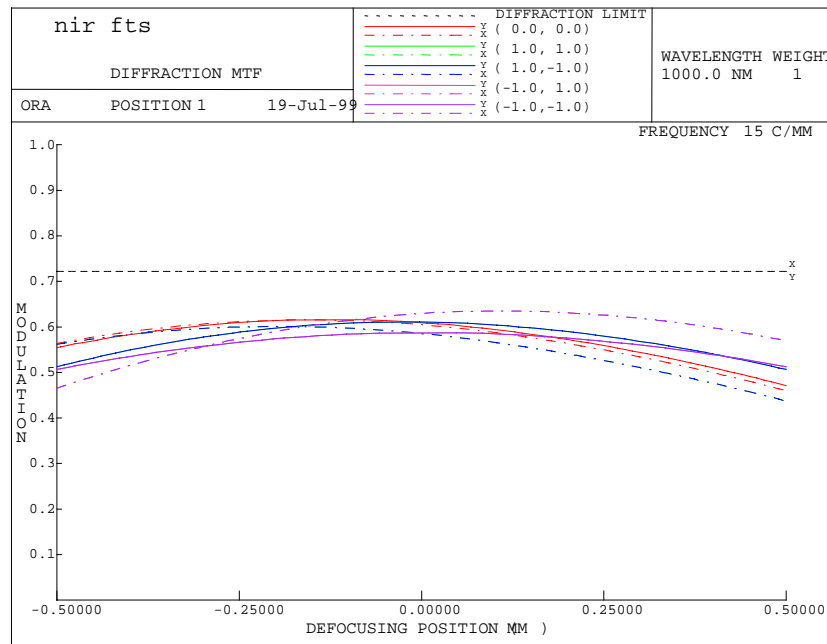


Figure 2.1-5: NIRCAM-FTS: Through-focus MTF calculated in center and corners of the field for a frequency of 15 cycles/mm.

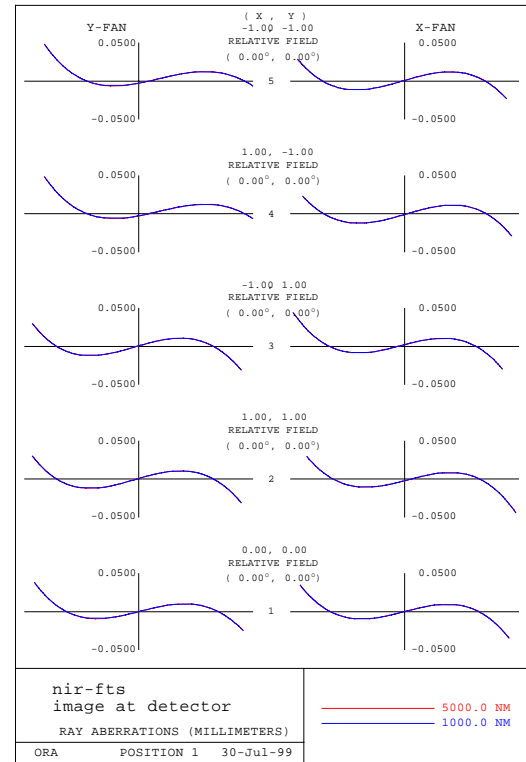
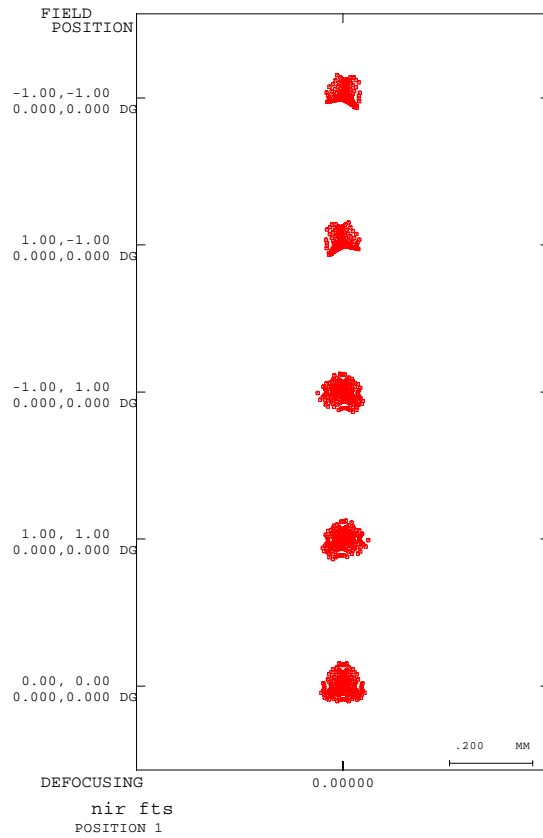


Figure 2.1-6 (left): NIRCAM – FTS: Geometric spot images at detector in center and corners of the field.

Figure 2.1-7 (right): NIRCAM – FTS: lateral aberrations at detector in center and corners of the field.

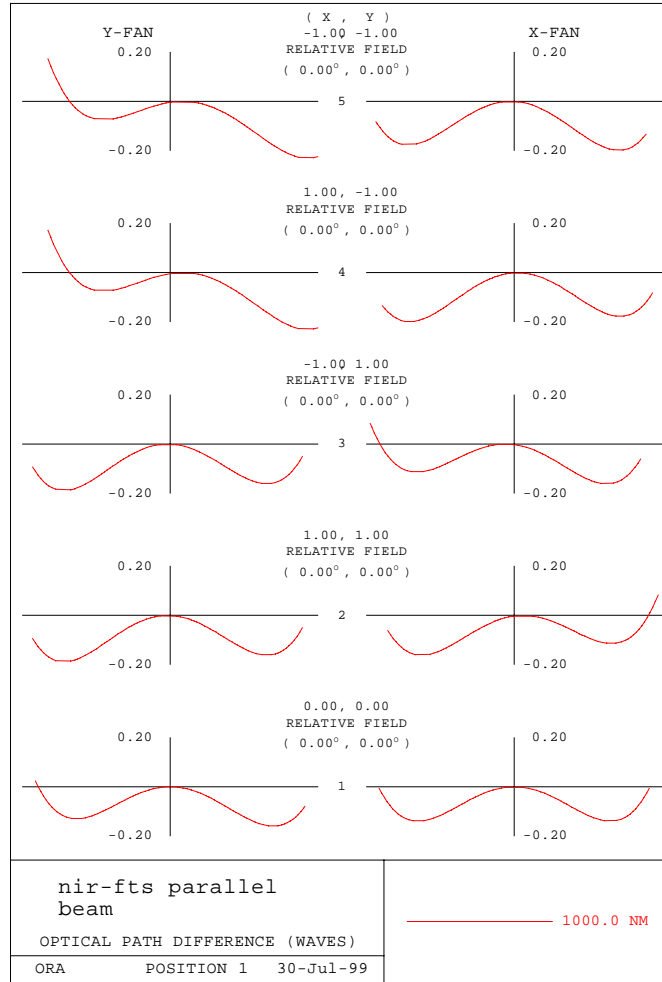


Figure 2.1-8: NIRCAM-FTS: quality of parallel beam (optical path differences) across the pupil.

Modulation Efficiency

The modulation efficiency is a measure of the contrast of the interference fringes. A value < 1 is caused by phase differences across the wavefronts of the two interfering beams, and has an effect on the instrument sensitivity.

The modulation efficiency is only affected by non-perfect components in the interferometer optical paths, where the two interfering beams are still separated, namely the beam-splitter, the beam-recombiner and the rooftops.

The reduction of the modulation efficiency is caused by wavefront shear and tilt, wavefront error and beamsplitter/ beam-recombiner performance.

According to /4/, the modulation efficiency is given by the following equation:

$$\eta_{\text{mod}}(\sigma) = \frac{\sin(\pi \cdot \sigma \cdot \theta \cdot \text{shear})}{\pi \cdot \sigma \cdot \theta \cdot \text{shear}} \cdot \frac{2 \cdot J_1(\pi \cdot \sigma \cdot D \cdot \text{tilt})}{\pi \cdot \sigma \cdot D \cdot \text{tilt}} \cdot e^{-2 \cdot (\pi \cdot \sigma \cdot \text{we})^2} \cdot 4 \cdot R(\sigma) \cdot T(\sigma)$$

σ = wavenumber [cm^{-1}]

θ = beam divergence of one resolution element (detector pixel) [rad]

shear = lateral shift of the two wavefronts [cm]

D = pupil diameter [cm]

tilt = tilt angle of the two wavefronts [rad]

we = rms wavefront roughness [cm]

R,T = beamsplitter reflectivity/transmission

Shear of wavefronts

Wavefront shear can have two causes:

- displacement of the rooftop in X-direction
- movement of the rooftop along Z-direction for OPD generation

Both effects cause a relative displacements of the two interfering wavefronts. Major phase differences between the two interfering wavefronts occur when the wavefront planarity is not good. The performance of the baseline design is uncritical in this respect (see Figure 2.1-9) and tolerates about 1 mm shear for 1% reduction in efficiency.

Tilt of wavefronts

A tilt of the two interfering wavefronts will cause a varying phase difference across the pupils. For a given tilt angle this phase difference increases with increasing pupil diameter. The pupil diameter of this design is rather large (100 mm), and therefore only small tilt angles are tolerable. This is the reason why in the baseline design one of the rooftops is used to compensate for tilt within the interferometer.

Wavefront error

Besides shear and tilt, a phase difference between the two interfering wavefronts can be caused by non-perfect optical surfaces. Most critical in this respect are the beamsplitter/beam-recombiner surfaces. The total wavefront error should be less than 30 nm rms in order to get > 95% modulation efficiency down to 0.6 μm . This can be achieved with surface planarities of about $\lambda/60$ rms.

Beamsplitter/beam-recombiner performance

Ideally the beamsplitter/beam-recombiner coatings should provide a 50:50 amplitude division of the input radiation. Major deviations of this beamsplitting ratio at certain wavelengths will reduce the modulation efficiency at these wavelengths. The

beamsplitter could be a thin gold coating on the CaF₂ substrate, which should provide a uniform transmission/reflection characteristic throughout the wavelength range. If this ratio can be kept within 45% and 55% then the resulting modulation efficiency is better than 0.99.

	Required performance	Modulation efficiency	Comment
Shear	< 1 mm	> 0.99	uncritical
Tilt	< 0.5 μ rad	> 0.99	in-orbit adjustment capability required
Wavefront error	< 30 nm rms	> 0.95	good beamsplitter planarity required
Beamsplitter	0.45 < R,T < 0.55	> 0.99	uncritical

Table 2.1-3: Proposed performance requirements to keep the modulation efficiency > 92% at 0.6 μ m

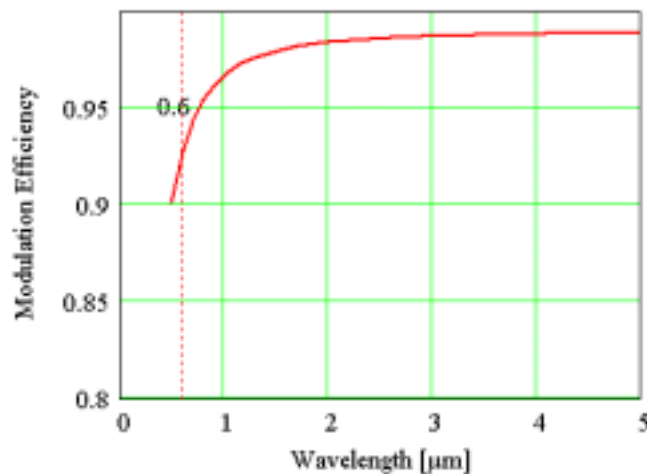


Figure 2.1-9: Modulation efficiency as function of wavelength, assuming above listed performance figures. Most critical is the wavefront error at short wavelengths because of its exponential characteristic.

Transmission

The optical transmission is wavelength dependent and is expected to be lowest at the shortest wavelength. At 1 μ m wavelength the following reflectivity figures are assumed:

- mean reflection of a gold coated mirror 0.98
- mean transmission of a broad band filter 0.93
- mean beamsplitter efficiency 0.97
- modulation efficiency at 1 μ m 0.96

The beamsplitter efficiency includes about 3% reflections at the non-coated surfaces; the absorption is assumed negligible.

In the interferometer mode the efficiency is reduced by a factor of 2, since only one output port is being used. The effect is equivalent to a factor 2 lower transmission.

Including the modulation efficiency, the mean overall transmission at 1 μm is then:

Camera mode: $T \sim 0.75$

Interferometer mode: $T \sim 0.38$ (single port)

2.1.4 Photometric Performance

A photometric performance model has been established to simulate the expected in-orbit instrument performance. The model includes all efficiencies from the telescope transmission up to the detector quantum efficiency. As photon background the expected zodiacal light (ref. /5/) has been considered.

Figure 2.1-10 shows the magnitudes of point objects as a function of wavelength that can be resolved in camera and imaging FTS mode for 10^5 sec observation time and a Signal-to-Noise-Ratio (SNR) of 10.

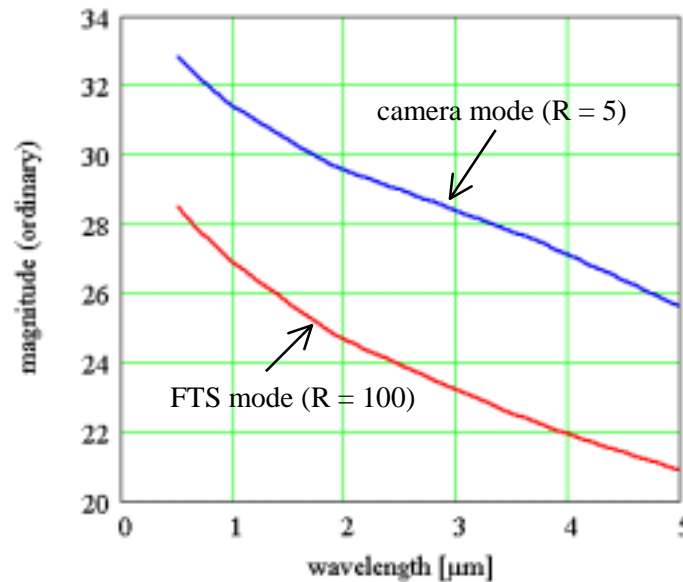


Figure 2.1-10: magnitude of point sources vs. wavelength that can be resolved in camera and IFTS mode with an SNR of 10 for an observation time of 10^5 sec (ordinary magnitudes!). In the FTS mode all 20 low spectral resolution elements within a broad band are recorded simultaneously.

Discussion of Results

The performance of the camera mode is for all target magnitudes photon noise limited. In the faint object limit of Figure 2.1-10 the zodiacal light is the dominating noise source. The detector and the readout noise are negligible.

The photon noise of the interferometer mode is comparable to the photon noise of the camera, since the whole target and background radiation within the selected broad band will reach the detector. Therefore, the performance of the IFTS is for all target magnitudes photon noise limited, and the detector and readout noise are negligible.

2.1.5 Opto-Mechanical Design

The baseline opto-mechanical designs are shown in Figure 2.1-11 and Figure 2.1-12.

The optical bench as primary structure consists of a light-weighted plate made of C/SiC material. The C/SiC brackets for the optical components are directly attached to the baseplate. The mirrors are connected to the brackets by an isostatic 3 point support. Flexible INVAR mounts are used as connection elements.

The two folding mirrors are mounted on a separate C/SiC plate which can be moved by a mechanism for optics refocusing.

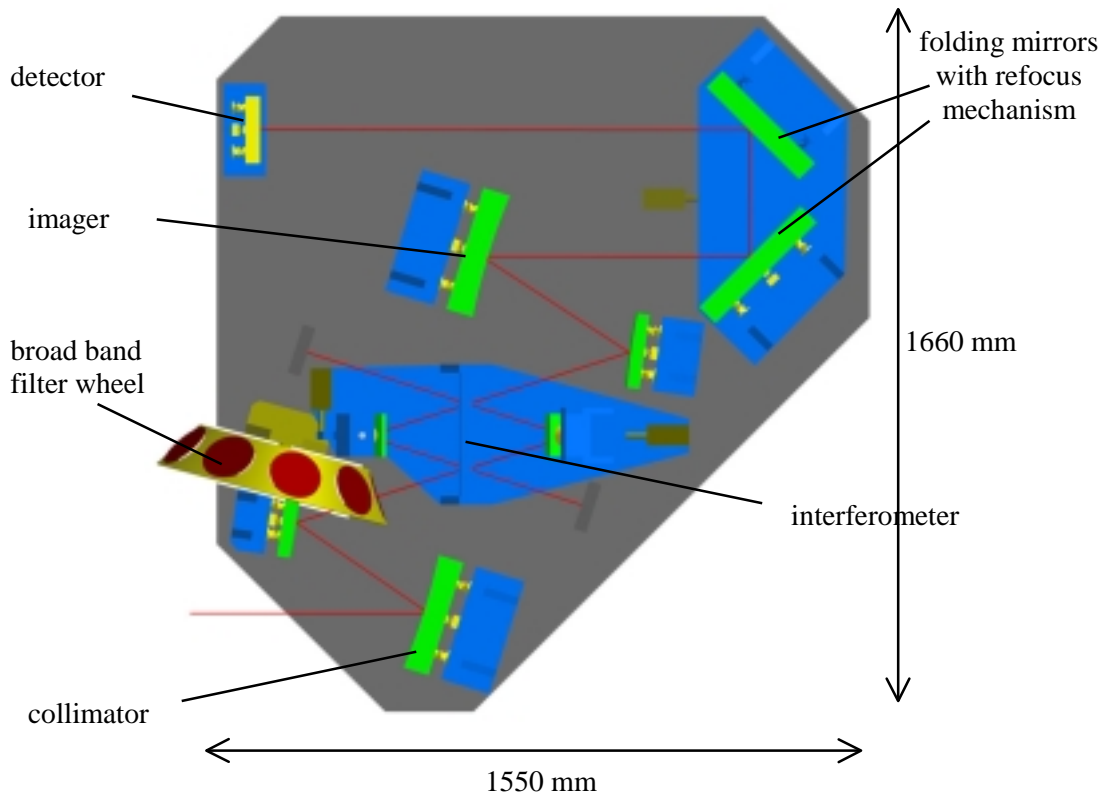


Figure 2.1-11: NIRCAM - FTS design: top view

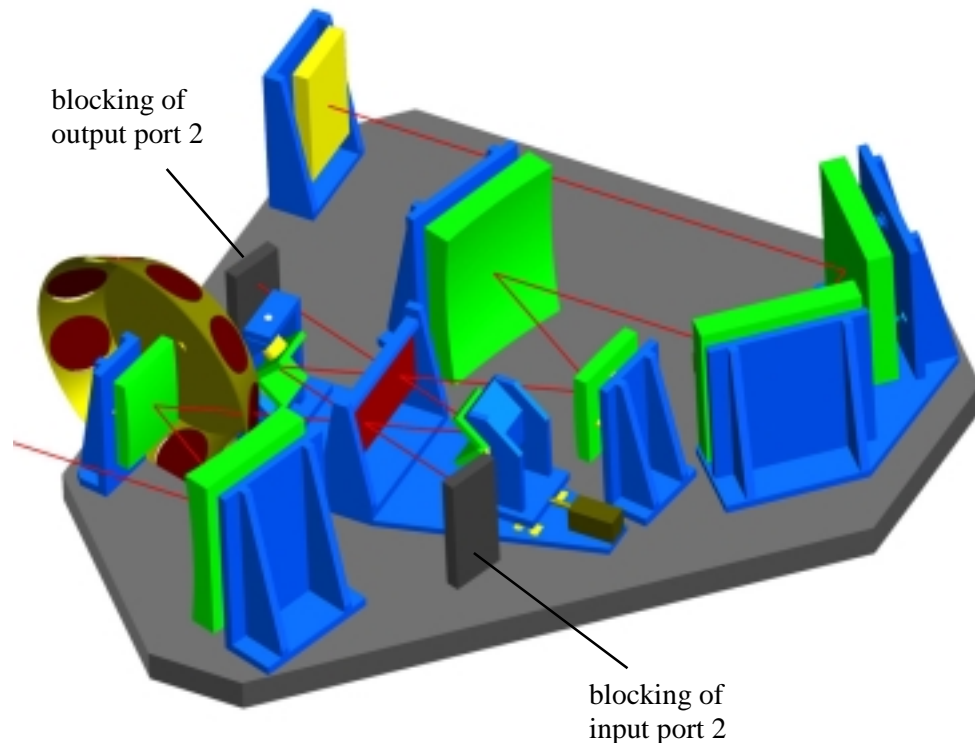


Figure 2.1-12: NIRCAM - FTS design: 3D view

2.1.6 Budgets

The overall dimensions are: 1.66 x 1.55 x 0.58 m³

The estimated overall mass of the Imaging FTS is 88 kg (Table 2.1-4).

	Mass [kg]
Primary structure	40
Bracketts, mounts, filter wheel	17.5
Optical components	19.5
Mechanisms	1
Miscellaneous (I/F bracketts, harness, etc.)	10
Total	88

Table 2.1-4: NIRCAM - FTS mass budget

2.1.7 *Conclusions*

The presented design of an Imaging Fourier Transform Spectrometer in the near infrared has very good imaging quality.

The interferometer optics is a rather compact Mach-Zehnder configuration which – given the small stroke of the moving mirror and the good quality of the interfering optical beams - works well as a Fourier Transform Spectrometer. This rather compact interferometer optics consists of planar surfaces only and can be built and tested as a separate module.

Possible criticalities concerning a reduction in modulation efficiency arise from a tilt of the optical components and the planarity of the beamsplitter surface (wavefront error). The use of rooftops as retro-reflectors reduce the critical tilt axes to one, which is adjustable in-orbit. As the interfering beams are very parallel, shear is not critical.

The main IFTS features are:

- + one optical configuration for 2 modes: a camera mode and a spectrometer mode
- + high image quality in camera and spectrometer mode
- + high spectral quality; easy spectral calibration (achromatic interferometer optics, all spectral information on the same detector pixel)
- + low sensitivity against detector noise, internal straylight and particle impact (after FFT the signal offset is distributed across all spectral elements)
- + compact interferometer of high stability => simple OPD measurement system
- low efficiency in case not all spectral information within a broad band is needed (this would require additional filtering)

Possible improvements:

- + enhancement possibility to also use the second output port

The following work is recommended for the next study phase:

- o filter definition and design
- o the necessity of an active adjustment provision for the rooftops
- o investigation of expected maximum optics defocusing (need of refocusing mechanisms)

2.2 Critical Areas and Recommended Development Activities

2.2.1 Instrument Hardware Breakdown

Figure 2.2-1 shows the HW breakdown of the filter wheel camera. The shaded boxes provide an overview of potential critical subsystems or of subsystems containing critical elements as listed in chapter 2.2.2.

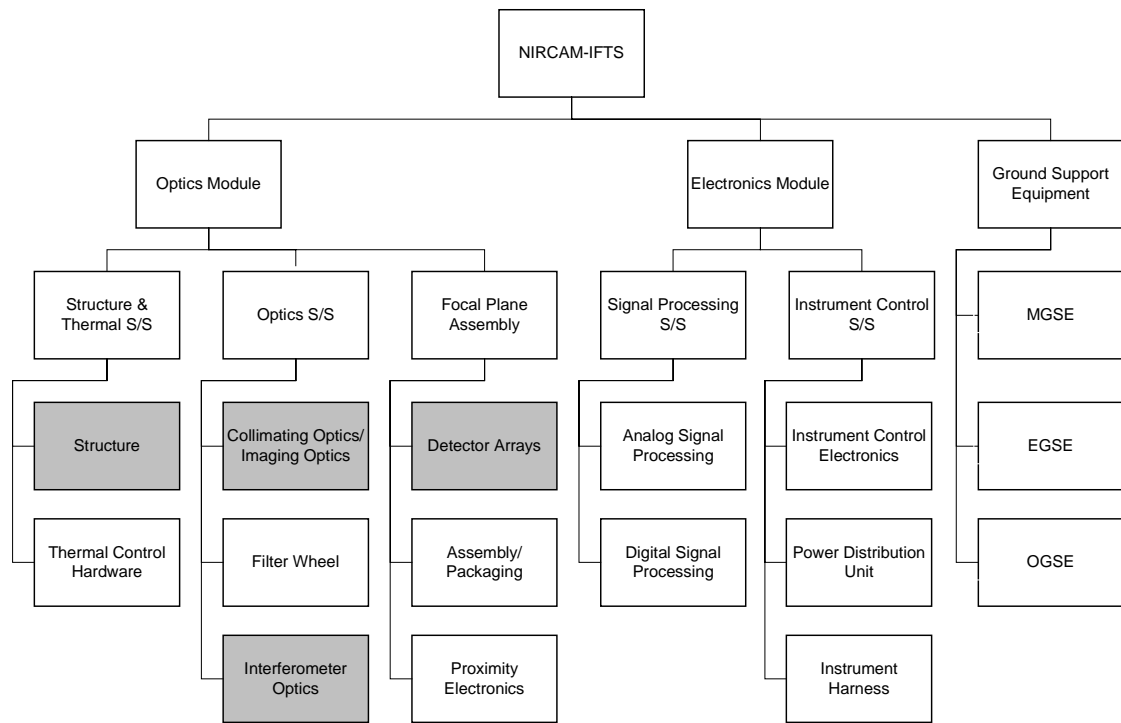


Figure 2.2-1: Instrument Hardware Breakdown; shaded areas indicate potential critical subsystems.

2.2.2 Critical Areas and Technology Requirements

Potential criticalities to be considered during the development of the instruments are

- items whose failing may affect the satellite performance or survival probability
- single point failures and non-redundant major elements
- items whose failing/degradation may affect the instrument performance
- items not previously space qualified
- items with exceptional process sensitivity and long lead items

The critical areas of the NIRCAM-FTS are mainly concerned with the last two items, i.e. subsystems which contain new technologies or technologies of expected long development duration. These technologies should be identified in an early stage of the project to allow definition of a dedicated technology development program in order to reduce the development risks of the project.

Critical Areas and Risks

In ref. /3/ a generic list of critical areas had been provided, which is valid for all instruments under consideration. Instrument specific areas of potential criticality for NIRCAM-FTS are summarized in the following Table 2.2-1.

Subsystem	Critical area	Comments
imaging/ collim. optics	large aspherical mirrors	require special manufacturing tools
interferometer	mechanical OPD measurement	requires high structural stability
	OPD mechanisms	guidance precision
	performance and mounting of beamsplitter	difference in CTE

Table 2.2-1: Potential critical areas of NIRCAM-FTS

Technology Requirements

The imaging and collimating optics consist of relatively large aspherical mirrors, but these can be manufactured with state-of-the-art tools. Breadboarding is not considered necessary, but this technology will require careful planning of resources.

Using mechanical OPD sensors, the function of this approach needs to be verified in an early stage of development. Alternative solution was the use of an optical reference, which would then also be a critical item (qualification of an LED). A good guidance precision of the flexible hinges will lower the performance criticality of the interferometer and should also be breadboarded.

The beamsplitter has a different CTE than the instrument structure, and its stability and performance at low temperatures should also be demonstrated in an early stage of the project. The beamsplitter needs to be mounted in a way which avoids stress during cool-down and which will survive the launch loads.

2.2.3 Recommended Follow-On Activities

Technology Development Activities on Instrument Level

In order to minimize the development risks the following technology development activities are recommended.

- verification of C/SiC material for structural and optical components
- verification of the interferometer concept (OPD measurement, mechanisms and beamsplitter mounting and performance)

For each of these activities, the following technology development activities are proposed:

- critical review of existing technologies
- design and manufacturing of a representative unit
- verification of performance prior to and after environmental tests, at ambient and at operating conditions

The expected duration of the development activities is 15 months.

Technology Development Activities on System Level

There are other technology verification activities which are considered necessary, especially the developments of the detectors and mechanisms for refocusing. But these technologies will be needed for other NGST hardware units as well and it is assumed that they will be developed on system level (under NASA contracts).

2.2.4 Technology Development Roadmap

The technology development roadmap for the major critical technologies is depicted in Figure 2.2-2 below.

The instrument specific hardware elements which are recommended for technology development are

- C/SiC material at cryogenic conditions
- filter wheel mechanisms and filter mounting

The system level hardware elements that are recommended for technology development are (corresponding developments activities are on-going)

- large and low noise detectors
- actuators/mechanisms for refocusing

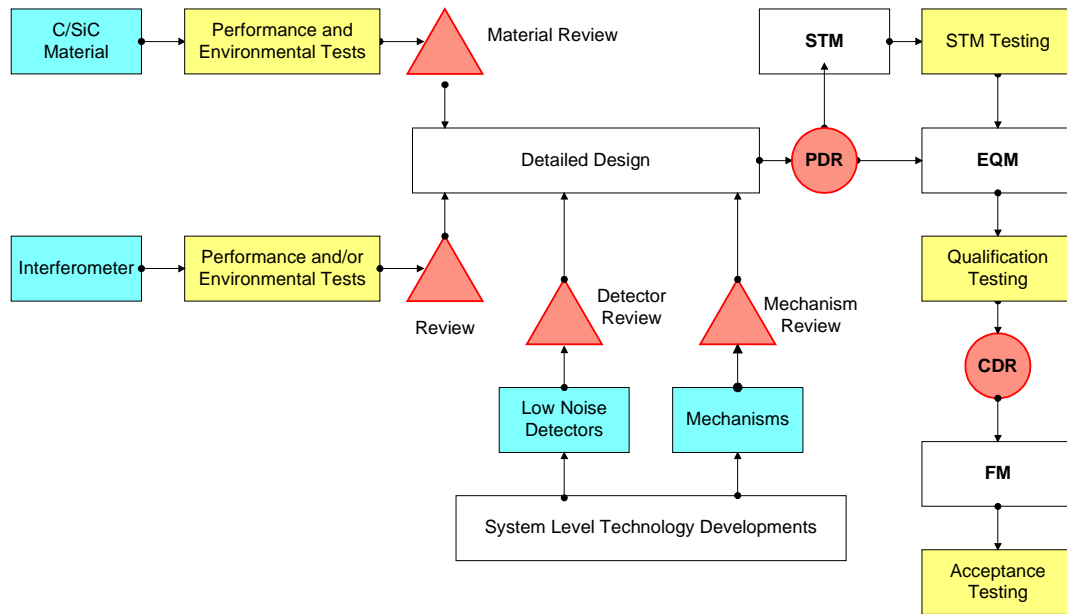


Figure 2.2-2: Technology Development Roadmap

2.3 Development Planning for Phases B and C/D

2.3.1 Work Breakdown Structure

The function oriented Work Breakdown Structure (WBS) is shown in Figure 2.3-1 below. The project is subdivided in management, product assurance, engineering, MAIT and procurement tasks. This WBS and the hardware breakdown shown in Figure 2.2-1 form the basis for the industrial cost estimate.

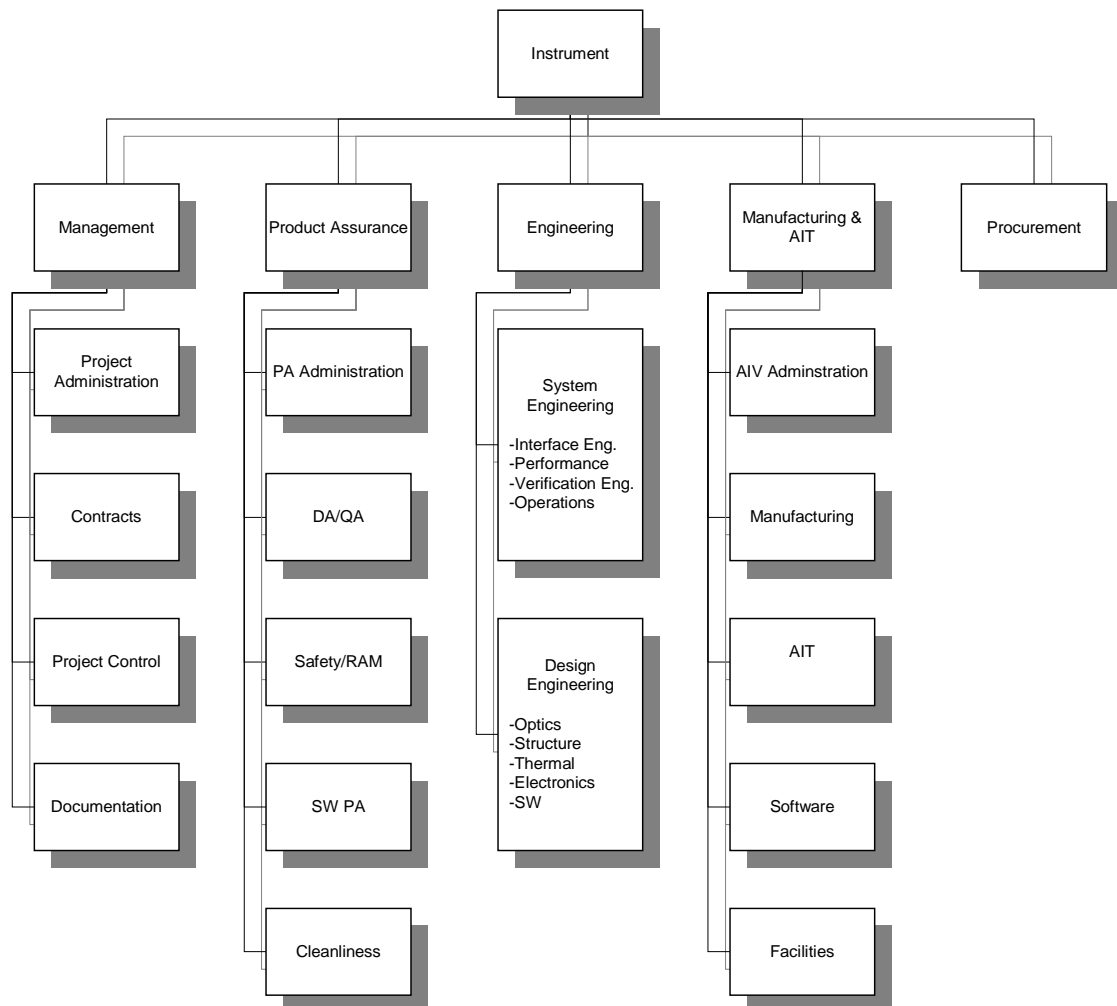


Figure 2.3-1: Function oriented Work Breakdown Structure

2.3.2 *Development Planning*

Two model philosophies have been considered for Phases B and C/D:

- **Standard Model Philosophy** (or standard development approach), according to a typical ESA space project and aiming for low risk
- **Alternative Model Philosophy** (or alternative development approach), trying to meet the NASA schedule

Standard Model Philosophy and Schedule

The standard philosophy is based on a typical (European) space project approach and shown in Figure 2.3-2. The development risk is minimized by building a set of prototypes and models: any design deficiencies identified on a lower level model can be eliminated on the subsequent higher level model. The sequential flow of models and associated learning steps will minimize potential risks for the flight model.

Besides technology breadboards and prototypes the following models are envisaged:

- Structural/Thermal Model (STM)
- Engineering Qualification Model (EQM)
- Flight Model (FM)
- Flight Spare

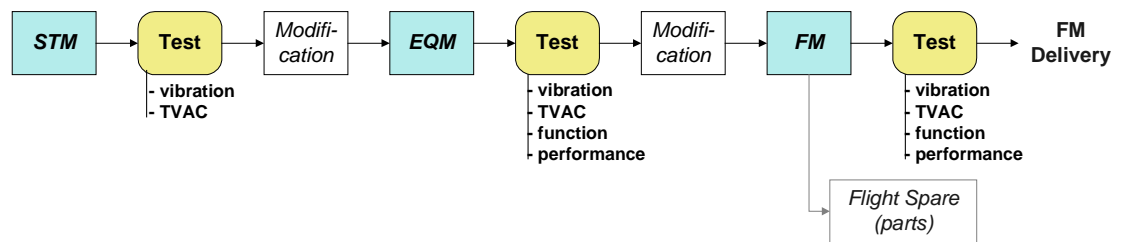


Figure 2.3-2: Standard Model Philosophy

The STM will be used to test the structural and thermal performance at low temperatures and after launch loads. Likely design modifications for the EQM will be derived. The STM will then be shipped to NASA for system level tests.

The EQM will be fully equipped and will undergo all performance and environmental tests on qualification levels. Design modifications for the FM will be derived, if necessary. The FM will be tested to acceptance levels only. The flight spare will consist of a set of instrument functional units and spare parts.

Drawback of this approach is the long development duration: the FM delivery will not be before end of 2007, see Figure 2.3-4. This delivery date is about 1.5 years later than scheduled by NASA.

Advantage of this approach is the identification of hardware problems at the earliest possible stages. This will allow to implement necessary design modifications and reduce the risk for the flight model performance.

Alternative Model Philosophy and Schedule

In order to meet the NASA need dates for the NGST instruments, the above presented „standard“ schedule has to be reduced in time. This will lead to a reduction of models and a corresponding increase of risk.

Besides technology breadboards and prototypes, the following models are proposed:

- Structural/Thermal Model (STM)
- Optical Engineering Model (OEM)
- Proto-Flight Model (PFM)
- Flight Spare

The alternative model philosophy is shown in Figure 2.3-3 below.

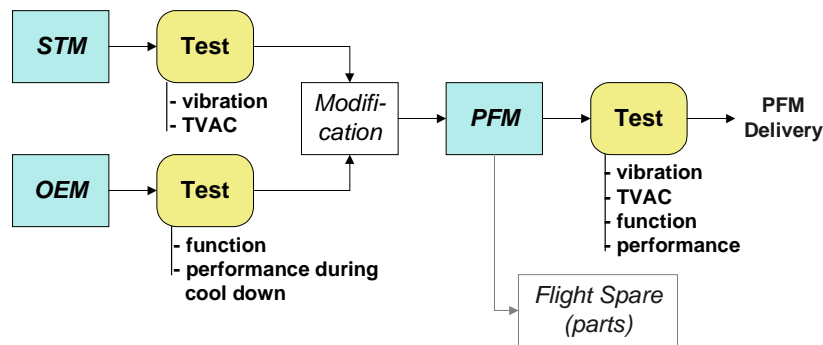


Figure 2.3-3: Alternative (NASA compatible) Model Philosophy

Even with a reduced development program the STM is still considered mandatory to test the performance of the large instrument structure at low operating temperatures and after launch loads. Necessary design modifications are likely and will be derived for the PFM. After testing, the STM will be shipped to NASA for system level tests.

In parallel to the STM, an OEM will be equipped such that an opto-mechanical (and electrical) verification of the concept can be performed at ambient temperature and at moderately lowered temperatures. The OEM will undergo an accelerated performance and environmental test program. It cannot be expected that the OEM will provide satisfying performance at operational temperature, but its behavior during cool-down, together with the STM test results, will provide valuable inputs for PFM improvements.

The PFM will be the first instrument model to be fully tested at acceptance levels. The flight spare will consist of a set of instrument functional units and spare parts.

Major drawbacks of this approach are:

- the final impacts of the structural/ thermal and opto-mechanical modifications can not be clarified before PFM availability
- the first real optical verification of the instrument will be performed on the flight model

Although with this alternative approach the associated risk is higher than for the standard model philosophy, it nevertheless bears the potential to meet the requested NASA need dates.

2.3.3 Schedule

The development schedule for both the standard and the NASA compatible approach are shown in Figure 2.3-4.

Up to and including Phase B the schedules are identical. However, the short PFM delivery date of the NASA compatible approach has repercussions not only on the shorter procurements phase but also on previous phases. In this case the technology readiness should be ensured at the beginning of Phase B and all manufacturing files should be finished at PDR (end of Phases B) in order to allow immediate start of hardware realization at the beginning of Phase C/D.

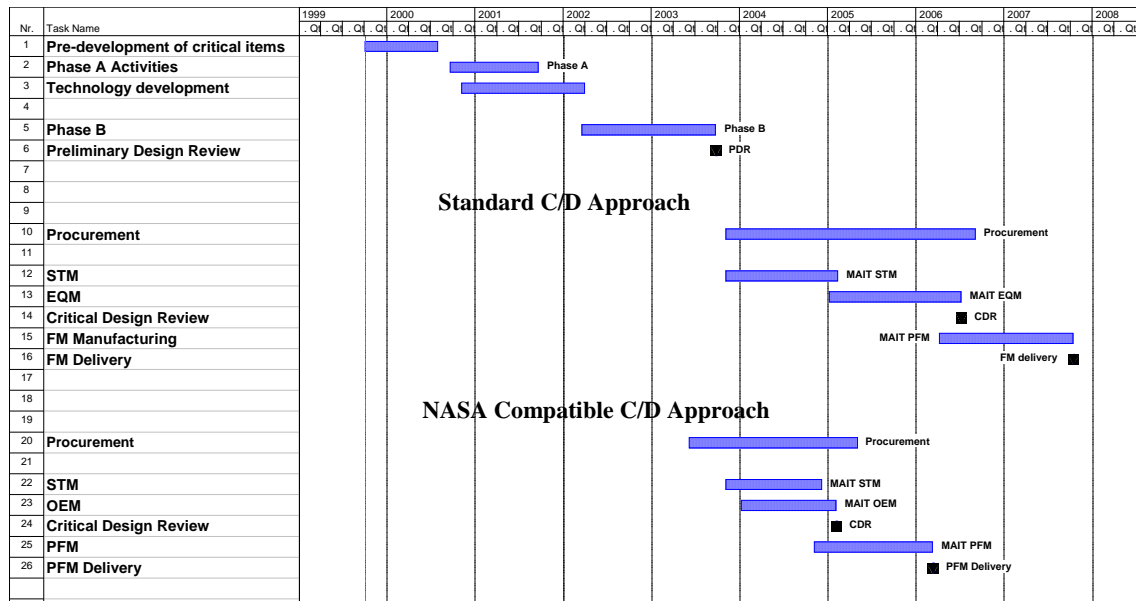


Figure 2.3-4: Proposed development schedule for both model philosophies

3 REFERENCES

- /1/ “Study of Payload Suite and Telescope for NGST”,
ESTEC/Contract no. 13111/98/NL/MS
- /2/ Statement of Work for “Study of Payload Suite and Telescope for NGST”,
PF-NGST-SOW-002, Issue 1, 24-Apr-98
- /3/ “NGST Payload Study, General Design Considerations”,
NGST-DSS-WHRP-001, 01-Oct-99
- /4/ “Note on modulation for NGST”,
J.F. Legault, BOMEM, 18-Jul-99
- /5/ NASA Exposure Time Calculator